



LAWRENCE  
LIVERMORE  
NATIONAL  
LABORATORY

# Optical constants of magnetron sputtered boron carbide thin films from photoabsorption data in the range 30 to 770 eV

R. Soufli, A. L. Aquila, F. Salmassi, M. Fernandez-Perea, E. M. Gullikson

May 29, 2008

Applied Optics

## **Disclaimer**

---

This document was prepared as an account of work sponsored by an agency of the United States government. Neither the United States government nor Lawrence Livermore National Security, LLC, nor any of their employees makes any warranty, expressed or implied, or assumes any legal liability or responsibility for the accuracy, completeness, or usefulness of any information, apparatus, product, or process disclosed, or represents that its use would not infringe privately owned rights. Reference herein to any specific commercial product, process, or service by trade name, trademark, manufacturer, or otherwise does not necessarily constitute or imply its endorsement, recommendation, or favoring by the United States government or Lawrence Livermore National Security, LLC. The views and opinions of authors expressed herein do not necessarily state or reflect those of the United States government or Lawrence Livermore National Security, LLC, and shall not be used for advertising or product endorsement purposes.

# **Optical constants of magnetron sputtered boron carbide thin films from photoabsorption data in the range 30 to 770 eV**

**Regina Soufli<sup>1</sup>, Andrew L. Aquila<sup>2</sup>, Farhad Salmassi<sup>2</sup>, Mónica Fernández-Perea<sup>3</sup>,**

**Eric M. Gullikson<sup>2</sup>**

<sup>1</sup>Lawrence Livermore National Laboratory, 7000 East Avenue, Livermore, CA 94550

<sup>2</sup>Lawrence Berkeley National Laboratory, 1 Cyclotron Road, Berkeley, CA 94720

<sup>3</sup>Instituto de Física Aplicada-Consejo Superior de Investigaciones Científicas, C/ Serrano 144,  
28006 Madrid, Spain

## **Abstract**

This work discusses the experimental determination of the optical constants (refractive index) of DC-magnetron-sputtered boron carbide films in the 30-770 eV photon energy range.

Transmittance measurements of three boron carbide films with thicknesses of 54.2, 79.0 and 112.5 nm were performed for this purpose. These are the first published experimental data for the refractive index of boron carbide films in the photon energy range above 160 eV, and for the near-edge x-ray absorption fine structure (NEXAFS) regions around the boron K (188 eV), carbon K (284.2 eV) and oxygen K (543.1 eV) absorption edges. The density, composition, surface chemistry and morphology of the films in this manuscript were also investigated using Rutherford Backscattering (RBS), X-ray Photoelectron Spectroscopy (XPS), Atomic Force Microscopy (AFM), Scanning Electron Microscopy (SEM), and extreme ultraviolet (EUV) reflectance measurements.

# 1. Introduction

In the past twenty years, boron carbide films with thicknesses ranging from a fraction of a nanometer to several nanometers have been implemented as constituent layers and interface barrier layers in reflective multilayer optics operating at photon energies from a few tens eV (EUV region) to hundreds keV (hard x-ray region) for use in instrumentation for solar physics, synchrotron radiation, EUV lithography and x-ray astronomy. The use of single-layer boron carbide films as reflective elements in the EUV region was first explored by Blumenstock *et al.*<sup>1,2</sup> More recently, boron carbide was proposed as a candidate reflective coating in the 0.08-2 keV range for the x-ray mirrors of the Linac Coherent Light Source (LCLS)<sup>3,4</sup>, the first x-ray free-electron laser (FEL) facility in the world, anticipated to begin its operation in 2009. Boron carbide is among the few materials that are expected to survive the extremely high peak brightness (higher by a factor of  $10^{10}$  than current 3<sup>rd</sup> generation synchrotron sources) of the LCLS FEL beam after it leaves the undulator enclosure. In the EUV/x-ray region, the photon energy-dependent refractive index  $n$  of materials is a complex number expressed as

$$n = 1 - \delta + i\beta \quad (1)$$

where  $1 - \delta$  and  $\beta$  represent the dispersive and absorptive portions of the refractive index, respectively. The terms  $\delta$ ,  $\beta$  are known as the optical constants. Knowledge of the refractive index of materials used in EUV/x-ray optics is essential in order to understand and predict their performance, and yet there has been only a limited number of experimental studies of the refractive index of boron carbide thin films in the EUV/x-ray photon energy region<sup>5,6</sup>. It is especially surprising that there are no experimental data available in the literature for the refractive index of boron carbide thin films in the energy range above 160 eV, which includes the energy regions of the boron K (188 eV) and carbon K (284 eV) absorption edges. In these

energy regions, fine structure (NEXAFS) is expected to occur, which depends on material properties such as the micro-structure and chemical composition, which in turn can depend on a variety of parameters such as the deposition conditions of the film. Because NEXAFS can depend on subtle effects, it cannot always be calculated accurately through modeling and atomic approximations, especially for composite materials such as the boron carbide films in the present manuscript. A qualitative presentation of experimental NEXAFS spectra of sputtered and evaporated boron carbide films around the boron, carbon and oxygen K edges is found in Refs. 7, 8.

Compared to other techniques (such as reflectance, ellipsometry and interferometry) used for experimental determination of the refractive index of materials in the EUV/x-ray region, the transmittance/photoabsorption method has the advantages of (i) being relatively insensitive to top surface micro-roughness of the samples under study, (ii) any layer of contamination on the measured samples can be normalized out from the results, assuming it is identical on all measured samples and (iii) once free-standing films of the material under study are prepared, it is rather straightforward to obtain experimental data in an extended energy region. In this paper we are presenting transmittance measurements in the energy range 30-770 eV on free-standing boron carbide thin films of three different thicknesses. Sample preparation and instrumentation are discussed in Section 2. In Section 3 the measurements and resulting NEXAFS structure are discussed, the absorptive part  $\beta$  of the refractive index of the boron carbide films is obtained directly from the transmittance results and the dispersive part  $\delta$  is obtained through a Kramers-Krönig transformation.

## 2. Experiment

## *2.1 Sample preparation and characterization*

The boron carbide films discussed in this work were deposited using a DC-magnetron sputtering deposition system located at Lawrence Livermore National Laboratory (LLNL) and described in detail in Ref. 9. The base pressure was  $10^{-7}$  Torr and argon was used as process gas at a pressure of  $10^{-2}$  Torr during deposition. The substrates used to deposit the boron carbide films for the transmittance measurements were 100-mm diameter silicon wafers with (100) orientation and 525-550  $\mu\text{m}$  in thickness. Prior to boron carbide deposition, the silicon wafers were spin-coated with EUV2D<sup>TM</sup> photoresist (manufactured by Shipley Corporation) and subsequently baked at 120° C for 2 minutes. After boron carbide deposition, stainless steel support rings, 8 mm in diameter with a 3 mm diameter opening, were glued onto the coated wafers using acetone-resistant glue and the samples were then soaked in acetone for a few minutes. This process resulted in removing the boron carbide films from the substrate and in producing free-standing boron carbide films mounted on the support rings, with a 3-mm-diameter area available for transmittance measurements. This method has also been implemented in earlier work<sup>10,11</sup> to produce free-standing films.

Three different thicknesses of boron carbide were deposited for transmittance measurements: 54.2, 79.0 and 112.5 nm. The thicknesses were verified experimentally by measuring the EUV reflectance vs. incidence angle on each sample at 91.8 eV and by fitting the Kiessig interference fringes as shown in Fig. 1. The EUV reflectance measurements were performed at beamline 6.3.2. of the Advanced Light Source (ALS) at Lawrence Berkeley National Laboratory (LBNL), described in detail in Section 2.2. These measurements were performed on three boron carbide films made during a subsequent deposition run and using the same parameters as the films made

for the transmittance measurements, but on blank Si wafer substrates (without a photoresist layer). The run-to-run reproducibility of the deposition system is better than 0.1%. In this manner, the process of fitting the boron carbide film thickness is more straightforward and presumably should result in more accurate thickness values, without the photoresist layer causing additional interference in the EUV reflectance results. The overall accuracy of this method of estimating film thickness is  $\pm 1\%$ . The high-spatial frequency roughness of the top surface used in the fits of the EUV reflectance data in Fig. 1 were provided from atomic force microscopy (AFM) measurements of these samples at LLNL, and the roughness values were: 0.46 nm rms for the 54.2 nm-thick film, 0.60 nm rms for the 79.0 nm-thick film, and 0.82 nm rms for the 112.5 nm-thick film. The density and composition of the 112.5 nm-thick boron carbide film were measured using RBS measurements with 2.275 MeV  $\text{He}^{++}$  ions and backscattering angle of  $160^\circ$ , performed by Evans Analytical Group in Sunnyvale, California. The atomic composition was thus found to be 74% boron, 20% carbon and 6% oxygen, corresponding to a boron:carbon ratio of 4:1. This boron:carbon ratio is consistent with the stoichiometry of the sputtering target material, and with earlier results reported in the literature for sputtered boron carbide thin films<sup>2,12,13,14,15,16</sup>. The presence of oxygen is also consistent with earlier published results for sputtered boron carbide films<sup>2,13,17,18</sup> and pulsed-laser deposited boron carbide films<sup>19</sup>. The 6% oxygen in the current films is most likely coming from the boron carbide sputtering target (i.e: was incorporated during target fabrication), as opposed to oxygen being present in the environment during deposition. This is further supported by the observation that films of other materials made in the same deposition chamber under similar conditions and tested by RBS show only a fraction of a percent atomic oxygen concentration. The RBS-determined atomic composition of the boron carbide films was included in the reflectance fits shown in Fig. 1. The

density determined from the RBS measurements on the 112.5 nm-thick boron carbide film was  $2.28 \text{ g/cm}^3$ , which corresponds to 90% of the bulk density of a boron carbide crystal ( $2.52 \text{ g/cm}^3$ ). In addition to the EUV reflectance measurements shown in Fig. 1, the thickness of the 112.5 nm-thick boron carbide film used in the RBS measurements was also verified by cross-sectional Scanning Electron Microscopy (SEM) measurements, and the SEM-measured thickness was consistent with the fitted thickness of 112.5 nm in Figure 1, to within 0.7%. XPS measurements were also performed by Evans Analytical Group on the boron carbide films discussed in this manuscript. The photon energy of the x-ray source was 1486.6 eV (Al  $K_\alpha$  emission line), the analysis area was  $1.4 \times 0.3 \text{ mm}$ , and measurements were performed at three take-off angles ( $20^\circ$ ,  $45^\circ$  and  $90^\circ$  from the grazing direction) to probe different depths from the top surface. Curve fits of the boron peaks in the XPS data demonstrated the presence of three components. A component at  $\sim 188.6 \text{ eV}$  was attributed to boron as  $\text{B}_4\text{C}$ . A component at  $\sim 190 \text{ eV}$  was attributed to boron-depleted boron carbide, or elemental boron, or boron sub-oxide ( $\text{B}_2\text{O}_x$ , where  $x < 3$ ). The third component at  $191.6 \text{ eV}$  was attributed to an oxide such as  $\text{B}_2\text{O}_3$ . The boron (as  $\text{B}_4\text{C}$ ) and the carbon (as carbide) were found to be at 4:1 atomic ratio, consistent with the RBS results discussed above. The  $\text{B}_4\text{C}$  component was observed to increase with increasing take-off angle while the other two components decreased, consistent with a  $\text{B}_4\text{C}$  film contaminated with an overlayer of boron-depleted boron carbide, elemental boron, boron sub-oxide and  $\text{B}_2\text{O}_3$ . At  $90^\circ$  take-off angle with a depth of analysis  $\sim 9 \text{ nm}$ , the atomic composition as determined by XPS was 63.7% boron, 22% carbon, 13.4% oxygen, and trace amounts of nitrogen (0.6%), aluminum (0.1%) and silicon (0.1%). Large-Angle X-ray Diffraction (LAXRD) measurements performed at LLNL using an x-ray source at 8048 eV (Cu  $K_\alpha$  emission line) on the aforementioned boron carbide films did not produce any evidence of crystallinity (i.e:



characteristic peaks) thus indicating that the structure of the films is amorphous, or nanocrystalline. The XPS and LAXRD findings presented above are in agreement with earlier reports in the literature for boron carbide films deposited under similar conditions as the films in this manuscript.

## *2.2 Instrument*

The EUV reflectance measurements discussed in Section 2.1 and the transmittance measurements discussed later in Section 3 were performed at beamline 6.3.2. of the ALS synchrotron at LBNL. The general characteristics of the beamline have been described in detail earlier<sup>20,21</sup>. The sample chamber allows translation of the sample in three dimensions, tilt in two dimensions and azimuth rotation of the sample holder. The available detectors include photodiodes and a CCD camera (the latter for sample alignment), which can be rotated 360° around the axis of the chamber.

For the transmittance measurements discussed in Section 3, four gratings (80, 200, 600 and 1200 lines/mm) were used in the monochromator to access the photon energy range from 30 to 770 eV. The monochromator exit slit was set to a width of 40  $\mu\text{m}$ . Photon energy calibration was based on the absorption edges of a series of filters (Al, Si, Ti, Cr) with a relative accuracy of 0.011% rms, and could be determined with 0.007% repeatability. During the measurements, 2<sup>nd</sup> harmonic and stray light suppression was also achieved with a series of transmission filters (Mg, Al, Si, Be, B, C, Ti, Cr, Co). For higher-order harmonic suppression, an “order suppressor” consisting of three mirrors at a variable grazing incidence angle (depending on energy range) and based on the principle of total external reflection was used in addition to the filters. The ALS storage ring current was used to normalize the signal against the storage ring current decay. The

base pressure in the measurement chamber was  $10^{-7}$  Torr. The signal was collected on a Si photodiode detector with a  $10 \times 10\text{-mm}^2$  active area and acceptance angle of  $2.4^\circ$ , in the energy range from 30 eV to 440 eV. A GaAsP diode detector with a 2 mm diameter pinhole with acceptance angle of  $1^\circ$  was used in the energy range 440 eV to 770 eV. The reflectance results at 91.8 eV discussed in Section 3.1 and Fig.1 were obtained with the 200 lines/mm grating, a Be filter for 2<sup>nd</sup>-harmonic suppression, the order suppressor consisting of three carbon mirrors at  $10^\circ$  grazing angle of incidence, and the Si photodiode detector.

### 3. Results and discussion

Fig. 2 shows the transmittance measurement results on the three free-standing boron carbide films with thicknesses of 54.2, 79.0 and 112.5 nm, respectively. The methodology used in this manuscript has also been implemented and described in detail in earlier work<sup>10,11</sup>. The transmittance curves in Fig. 2 were obtained through the expression  $T = I / I_0$  for the transmittance  $T$  of the film at a given photon energy, where  $I$  is the intensity transmitted through the boron carbide film and  $I_0$  is the intensity of the incident photon beam. Transmittance measurements were obtained in steps ranging from 0.05 eV to 1.2 eV, depending on the energy range. Measurement reproducibility was better than 0.5%, mostly limited by beam positioning on each of the films, except for the energy regions 30-50 eV and around the carbon K edge (284 eV) where the reproducibility is estimated at  $< 2\%$ , limited by photon flux. The energy-dependent, linear absorption coefficient  $\alpha$  ( $\text{nm}^{-1}$ ) of the sputtered boron carbide material was obtained through the expression:

$$T = T_0 \exp(-\alpha x) \quad (2)$$

where  $x$  (nm) is the thickness of stoichiometric boron carbide and  $T_0$  is the transmittance from layers other than stoichiometric boron carbide that may be present on the boron carbide film surface. Given the XPS analysis results presented in Section 2.1, the top 6 nm on each side of the three boron carbide films were assumed to be carbon- and oxygen-rich layers, contributing to  $T_0$ . In this manner, a total thickness of 12 nm would be contributing to  $T_0$  on each film and was therefore subtracted from each film thickness. Thus, the values used for  $x$  in eq. (2) were 42.2, 67.0, and 100.5 nm, for each of the three films respectively. An example of the fitting procedure using eq. (2) for  $\alpha$  is shown in Fig. 3, for four different photon energies. In the plot of the measured transmittance  $T$  (on a logarithmic scale) vs.  $x$  at a given photon energy, the data points form a straight line whose slope is equal to  $\alpha$ . Furthermore, the point where the straight line intercepts the y-axis corresponds to the transmittance  $T_0$  at  $x=0$ , assuming that the thickness of the overlayer responsible for  $T_0$  is the same for all three samples used in the measurements. A plot of the results for  $T_0$  vs. photon energy derived with the above procedure is shown in Fig. 4, including a curve calculated to fit the experimental results for  $T_0$ , corresponding to a 12 nm-thick layer (the thickness assumed for the overlayers contributing to  $T_0$  as explained earlier in this section) consisting of 10% boron, 50% carbon and 40% oxygen (atomic), with a density of 2.0 g/cm<sup>3</sup>. The atomic composition obtained from the fitted curve is significantly higher in carbon and oxygen and lower in boron than the results obtained from XPS analysis on the top surface of the boron carbide film discussed in Section 2.1. This could be attributed to the fact that the XPS-analyzed boron carbide film was only exposed to ambient environment, while the boron carbide films used in the transmittance measurements were deposited on a photoresist-coated substrate and subsequently soaked and removed in acetone (see Section 2.1), which could have resulted in

photoresist residue and other hydrocarbons left on the surface of the free-standing boron carbide films.

Fig. 5 shows the experimental results for the linear absorption coefficient  $\alpha$  vs. photon energy, obtained from eq. (2) with the procedure outlined in Fig. 3. The experimental results are plotted side-by-side with the values for  $\alpha$  from the atomic data tables maintained by the Center for X-ray Optics (CXRO)<sup>22</sup> by combining the available data for boron, carbon, and oxygen, and by using the RBS-determined density ( $2.28 \text{ g/cm}^3$ ) and atomic composition (74% boron, 20% carbon and 6% oxygen) of the present boron carbide films. Fig. 5 reveals significant differences between the present experimental data and the values from the atomic data tables, especially -and predictably- in energy regions around the boron, carbon and oxygen K absorption edges. The experimental linear absorption coefficient of the boron carbide films in the region of the boron K edge displays a prominent NEXAFS feature centered near 200 eV that is a factor of 2 higher than the values derived from the atomic data tables. The feature around 200 eV is in qualitative agreement with x-ray absorption spectra on boron carbide films reported in Refs. 7,8 and could be assigned to  $\sigma^*$ -like states<sup>8,23</sup>. Extended fine structure is also present in the energy region between the boron and carbon K-edges; such structure has not been reported in earlier literature. The experimental data in all three K-absorption edge regions (boron, carbon, oxygen) in Fig. 5 demonstrate pre-edge peaks located 7-9 eV below the main peaks, that could be attributed to  $\pi^*$ -like states; for instance, similar pre-edge peaks at the carbon and oxygen K-edge regions of boron carbide films have been attributed to C=O  $\pi^*$  resonances<sup>8,23</sup>. Qualitatively similar spectra to those shown in Fig. 5 in the carbon and oxygen K-edge regions were also obtained in Ref. 13 using a parallel electron energy loss (PEELS) technique that was performed as part of Transmission Electron

Microscope (TEM) analysis in the column boundary region of magnetron sputtered boron carbide films. At photon energies well above the oxygen K-edge region, the present experimental data are in good agreement with the values calculated from the atomic data tables. The experimental values obtained on ion-beam sputtered boron carbide films by Blumenstock *et al*<sup>2</sup> in the photon energy range 6.2-30.5 eV are also included in Fig. 5, and they appear consistent with the present experimental data.

Figure 6 shows plots of the optical constants  $\delta$  and  $\beta$  that compose the refractive index according to eq. (1). The absorptive part  $\beta$  was determined directly from the experimental data for the linear absorption coefficient  $\alpha$  through the relation:  $\beta = \lambda\alpha/4\pi$ , and  $\delta$  was determined through calculations based on the Kramers-Krönig relationship<sup>24</sup>:

$$\delta(E) = -\frac{2}{\pi} P \int_0^{\infty} \frac{E' \beta(E')}{E'^2 - E^2} dE', \quad (3)$$

where  $E$  represents the photon energy (related to the wavelength  $\lambda$  by  $E = hc/\lambda$ ) and  $P$  denotes the Cauchy principal value of the integral. The data set used for the absorption  $\beta$  inside the integral of eq. (3) was composed of: (i) Experimental data from Blumenstock *et al.* in the region 6.2-30 eV, (ii) Experimental data from the present manuscript in the region 30-770 eV, (iii) Values from the CXRO atomic tables in the photon energy region 770-30,000 eV, (iv) Extrapolations to  $E=0$  and  $E= \infty$  in the rest of the spectrum.

## 4. Conclusions

Through photoabsorption measurements in the photon energy region 30-770 eV we have established a new data set for the optical constants of magnetron sputtered boron carbide films, including NEXAFS structure in the energy regions around the boron, carbon and oxygen K

absorption edges. The new data set will be used to model and predict more accurately the response of EUV/x-ray optics with boron carbide as one of their constituent materials.

## **Acknowledgements**

The authors are thankful to Jeff C. Robinson (LLNL) for assistance with the thin film deposition, Franklin J. Dollar (LBNL) for assistance with the EUV reflectance measurements, Sherry L. Baker (LLNL) for the AFM and SEM measurements, Cheng L. Saw (LLNL) for LAXRD measurements, and Richard Bionta, Michael J. Pivovarov and Donn McMahon (LLNL) for support. We thank Angela Craig, Bruce Rothman and Patrick Schnabel (Evans Analytical Group, Sunnyvale, California) for the XPS and RBS measurements. Financial support for Mónica Fernández-Perea was provided by Consejo Superior de Investigaciones Científicas (Spain) under the Programa I3P (Ref. I3P-BPD2004), partially supported by the European Social Fund. This work was performed under the auspices of the U.S. Department of Energy by Lawrence Livermore National Laboratory under Contract No. DE-AC52-07NA27344, and by the University of California Lawrence Berkeley National Laboratory under Contract No. DE-AC03-76F00098.

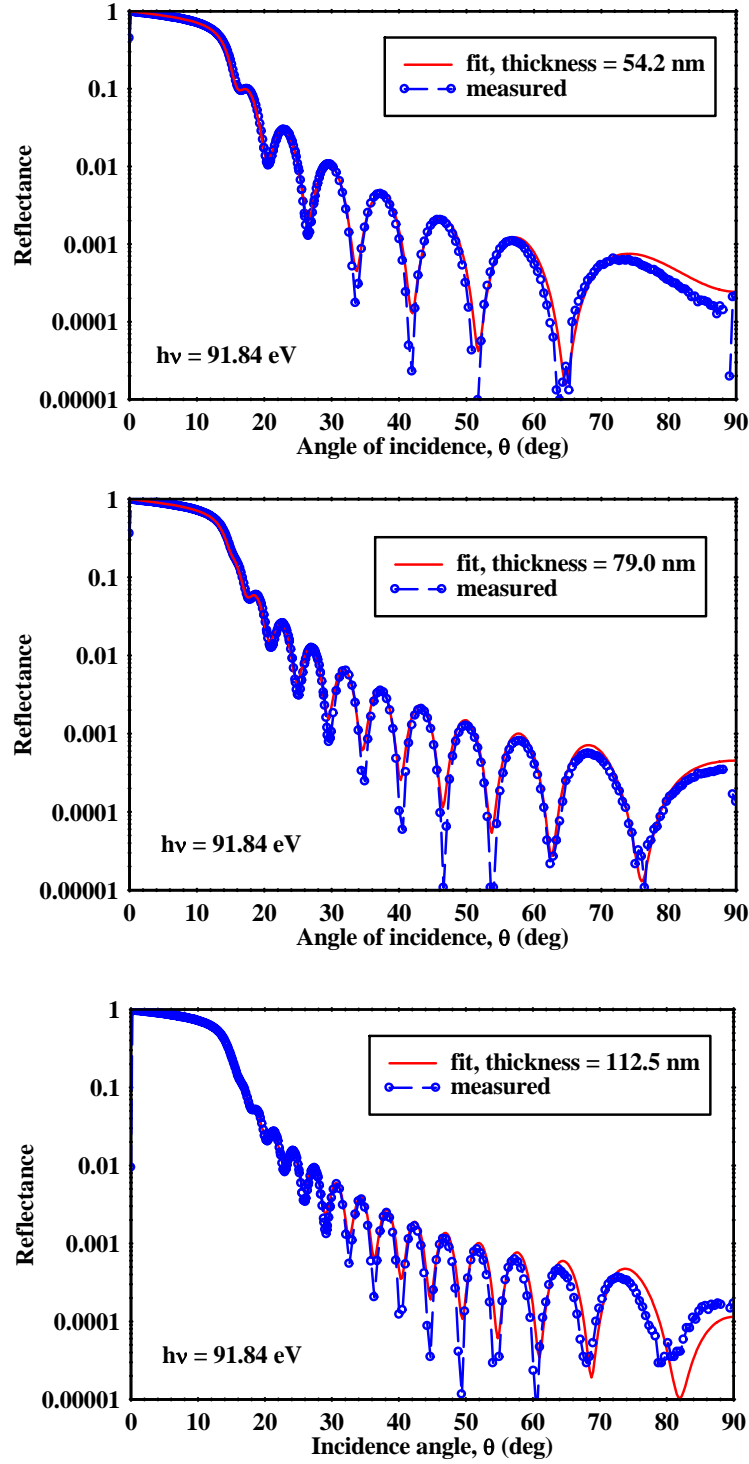


**Figure 1:** EUV reflectance data are fitted to determine the thickness for each of the three boron carbide films used in the transmittance measurements. The thickness of the 112.5 nm film was also verified with SEM measurements.

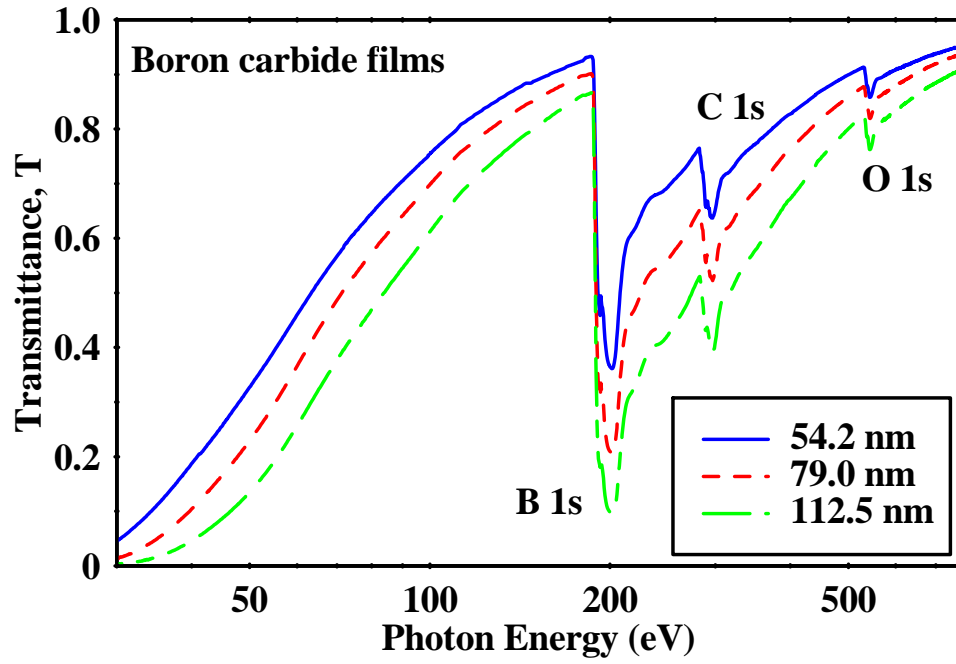


**Figure 2:** Experimental transmittance results from three free-standing boron carbide films. The prominent features seen in the three curves correspond to the boron, carbon and oxygen K (1s) absorption edges.



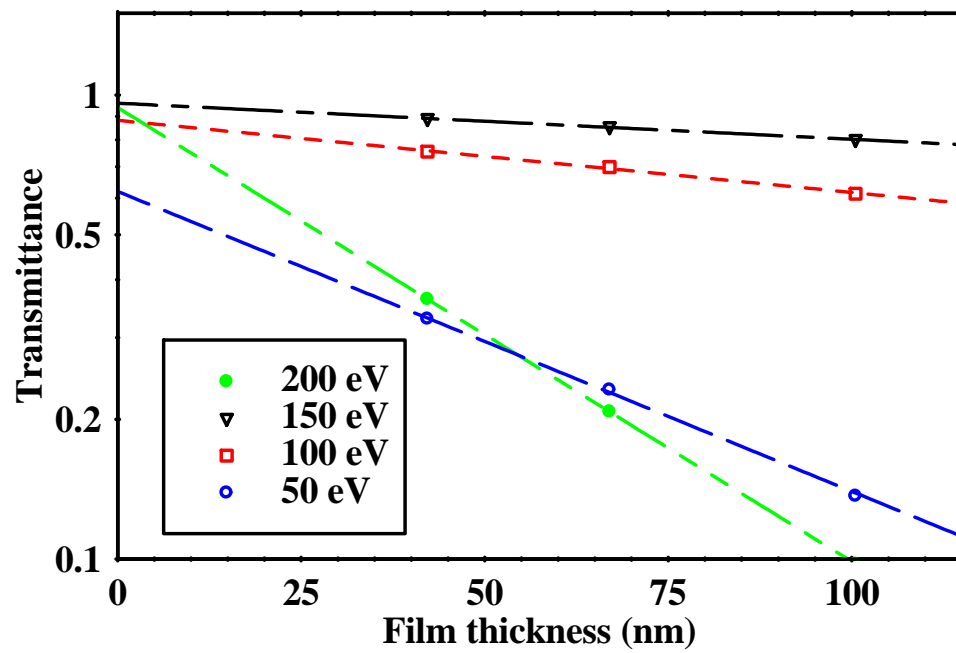


**Figure 3:** Fitted curves (dash lines) to experimental transmittance data from three boron carbide films (solid points) are shown at four photon energies.

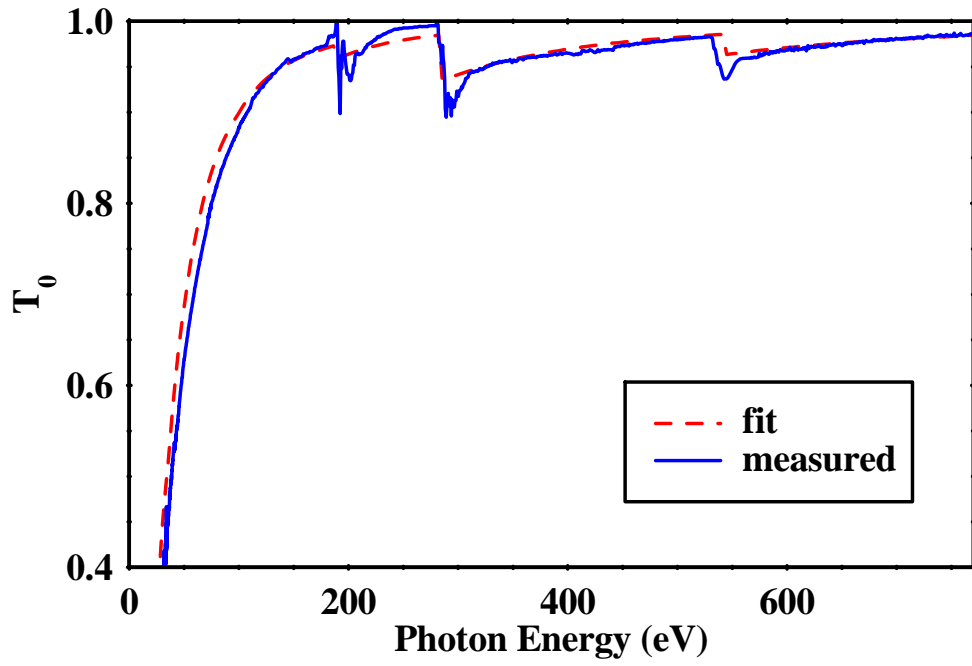


**Figure 4:** Experimental results (solid line) are shown for the transmittance  $T_0$  from overlayers of materials other than stoichiometric boron carbide. The dash line is a fit to the experimental results, using optical constants values for elemental boron, carbon and oxygen from the atomic data tables.

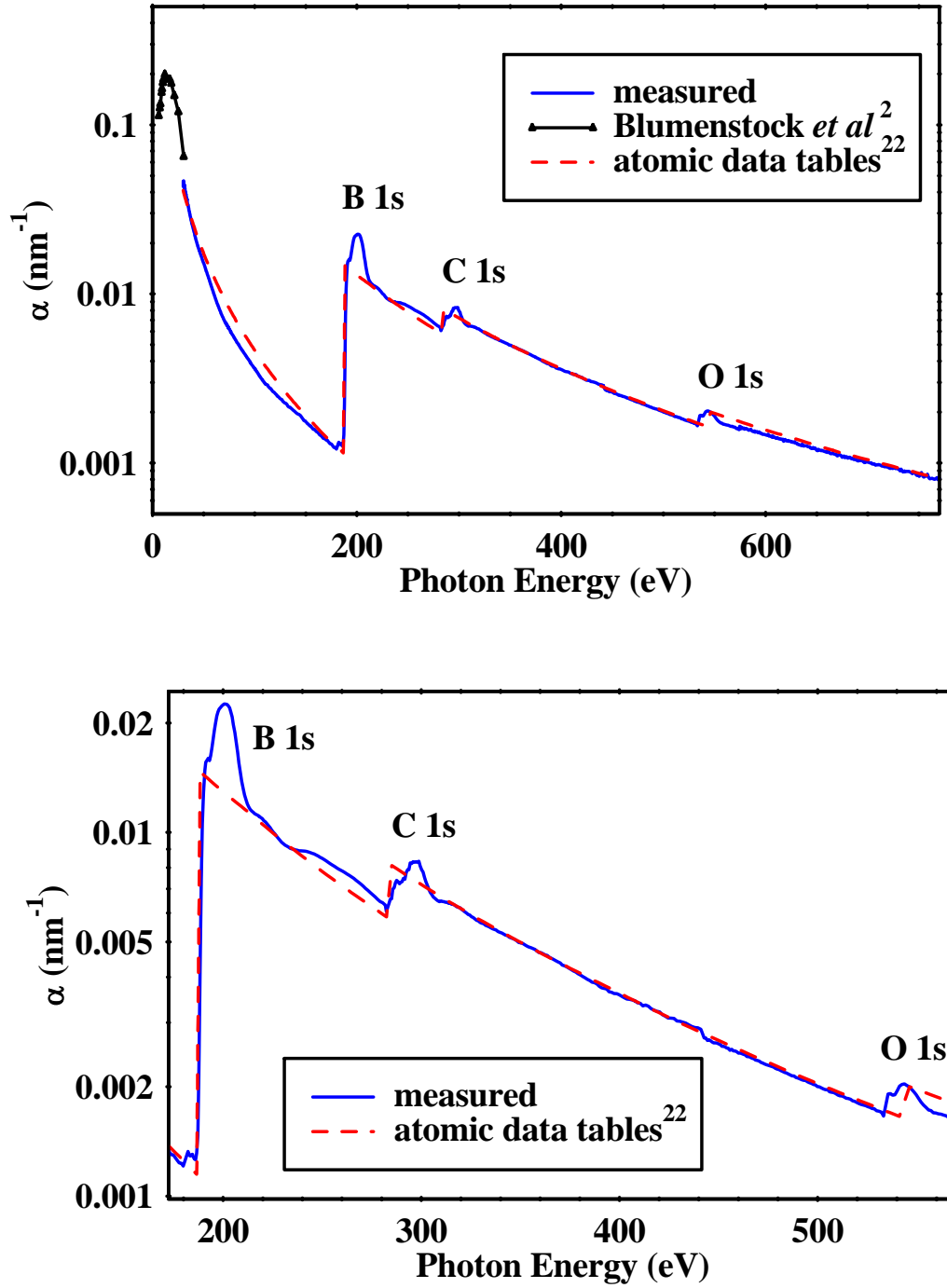


**Figure 5: Top:** Measured (solid line) and calculated (dash line) values for the linear absorption coefficient  $\alpha$  (log scale) of sputtered boron carbide. Experimental data in the energy range 6.2-30.5 eV by Blumenstock *et al.*<sup>22</sup> are also shown. **Bottom:** Expanded plots of  $\alpha$  (log scale) in the vicinity of the boron, carbon and oxygen K (1s) absorption edges.

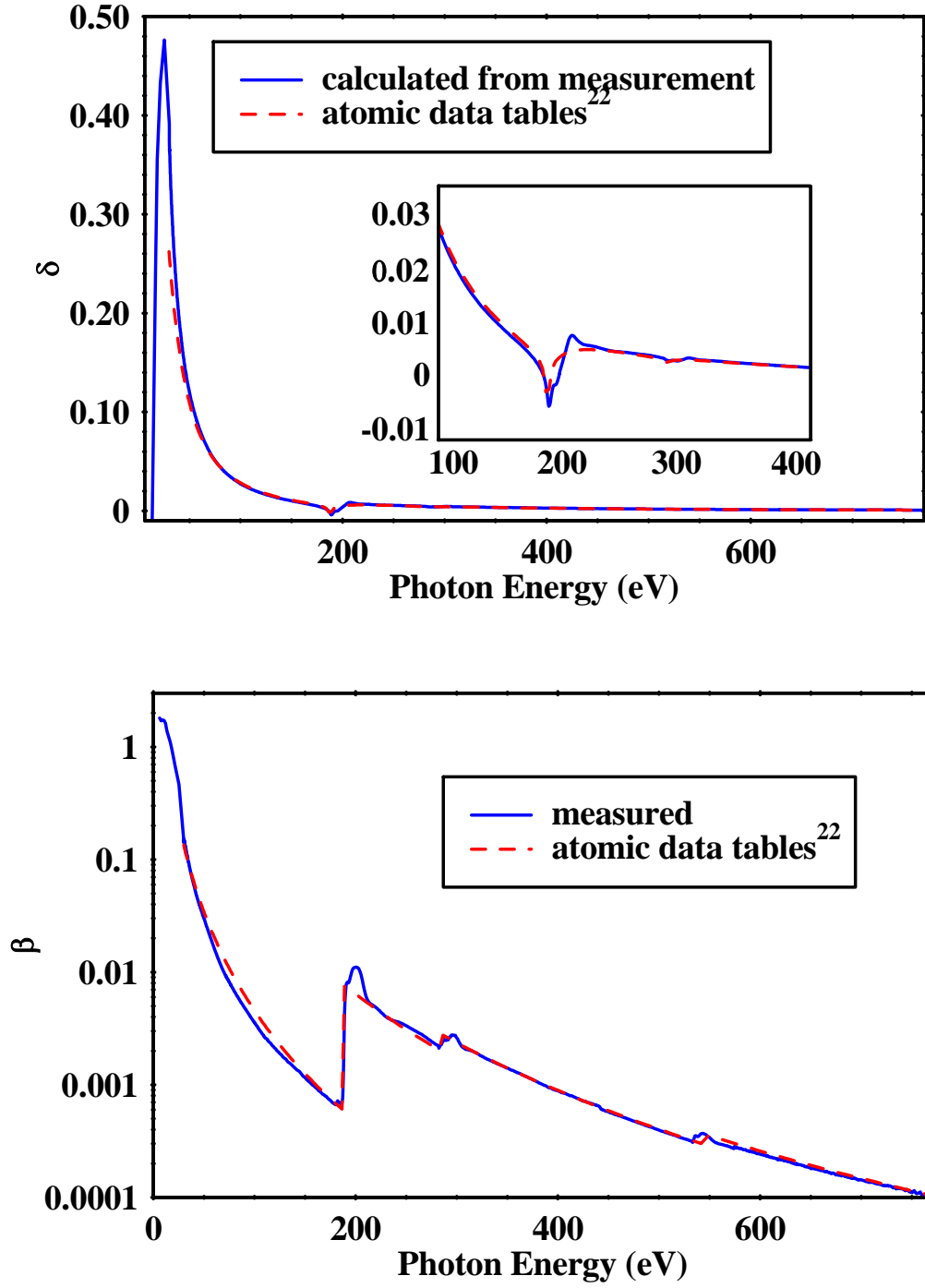


**Figure 6:** The optical constants  $\delta$  (top) and  $\beta$  (bottom, log scale) for sputtered boron carbide are plotted.  $\delta$  is calculated through the Kramers-Krönig relation, eq. (3), using a composite data set

of  $\beta$  values. The inset (top) shows an expanded plot of  $\delta$  in the energy region around the boron K edge.

## References

- <sup>1</sup> G. M. Blumenstock and Ritva A. M. Keski-Kuha, "Ion-beam-deposited boron carbide coatings for the extreme ultraviolet", *Appl. Opt.* **33**, 5962-5963 (1994).
- <sup>2</sup> G. M. Blumenstock, R. A. M. Keski-Kuha, and M. L. Ginter, "Extreme ultraviolet optical properties of ion-beam-deposited boron carbide thin films", *Proc. SPIE* **2515**, 558-564 (1995).
- <sup>3</sup> S. P. Hau-Riege, R. A. London, R. M. Bionta, *et al*, "Damage threshold of inorganic solids under free-electron-laser irradiation at 32.5 nm wavelength," *App. Phys. Lett.* **90**, 173128-1-3, (2007).
- <sup>4</sup> M. J. Pivovarov, R. M. Bionta, T. J. Mccarville, R. Soufli, and P. M. Stefan, "Soft X-ray Mirrors for the Linac Coherent Light Source", in *Advances in X-Ray/EUV Optics and Components II*, A. M. Khounsary, C. Morawe and S. Goto, eds., *Proc. SPIE* **6705**, 67050O, (2007).
- <sup>5</sup> C. Tarrio, R. N. Watts, T. B. Lucatorto, J. M. Slaughter, and C. M. Falco, "Optical constants of *in situ*-deposited films of important extreme-ultraviolet multilayer mirror materials", *Appl. Opt.* **37** 4100-4104 (1998).
- <sup>6</sup> J. I. Larruquet and R. A. M. Keski-Kuha, "Optical properties of hot-pressed B<sub>4</sub>C in the extreme ultraviolet", *Appl. Opt.* **39**, 1537-1540 (2000).
- <sup>7</sup> J.J. Jia, J.H. Underwood, E.M. Gullikson, T.A. Callcott, and R.C.C. Perera, "Soft X-ray Absorption Spectroscopy in 100 - 1000 eV region at the ALS", *J. of Electr. Spectr. Rel. Phenom.* **80**, 509-512 (1996).
- <sup>8</sup> J. Jimenez, D. G. J. Sutherland, T. van Buuren, J. A. Carlisle, L. J. Terminello, and F. J. Himpsel, "Photoemission and x-ray absorption study of boron carbide and its surface thermal stability", *Phys. Rev. B* **57**, 13167-13174 (1998).
- <sup>9</sup> R. Soufli, R. M. Hudyma, E. Spiller, E. M. Gullikson, M. A. Schmidt, J. C. Robinson, S. L. Baker, C. C. Walton, and J. S. Taylor "Sub-diffraction-limited multilayer coatings for the 0.3 numerical aperture micro-exposure tool for extreme ultraviolet lithography", *Appl. Opt.* **46**, 3736-3746 (2007).
- <sup>10</sup> E. M. Gullikson, P. Denham, S. Mrowka, and J. H. Underwood, "Absolute photoabsorption measurements of Mg, Al, and Si in the soft-x-ray region below the L<sub>2,3</sub> edges," *Phys. Rev. B* **49**, 16283-16288 (1994).
- <sup>11</sup> R. Soufli and E. M. Gullikson, "Absolute photoabsorption measurements of molybdenum in the range 60 to 930 eV for optical constant determination," *Appl. Opt.* **37**, 1713-1719 (1998).
- <sup>12</sup> M.-L. Wu, J. D. Kiely, T. Klemmer, Y.-T. Hsia, K. Howard, "Process-property relationship of boron carbide thin films by magnetron sputtering" *Thin Solid Films* **449**, 120-124 (2004).
- <sup>13</sup> T. Hu, L. Steihl, W. Rafaniello, *et al*, "Structures and properties of disordered boron carbide coatings generated by magnetron sputtering", *Thin Solid Films* **332**, 80-86 (1998).
- <sup>14</sup> C. I. Chiang, H. Holleck and O. Meyer, "Properties of RF sputtered B<sub>4</sub>C thin films", *NIM B* **91**, 692-695 (1994).
- <sup>15</sup> C. I. Chiang, O. Meyer, Rui M. C. da Silva, "The modification of mechanical properties and adhesion of boron carbide sputtered films by ion implantation", *NIM B* **117**, 408-414 (1996).
- <sup>16</sup> E. Pascual, E. Martinez, J. Esteve, A. Lousa, "Boron carbide thin films deposited by tuned-substrate RF magnetron sputtering", *Diamond and Related Materials* **8**, 402-405 (1999).
- <sup>17</sup> H.-Y. Chen, J. Wang, H. Yang, W.-Z. Li, H.-D. Li, "Synthesis of boron carbide films by ion beam sputtering", *Surface and Coatings Technology* **128-129**, 329-333 (2000).
- <sup>18</sup> C. Ronning, D. Schwen, S. Eyhusen, U. Vetter, H. Hofsäss, "Ion beam synthesis of boron carbide thin films", *Surface and Coatings Technology* **158-159**, 382-387 (2002).
- <sup>19</sup> W. J. Pan, J. Sun, H. Ling, N. Xu, Z.F. Zing, J. D. Wu, "Preparation of thin films of carbon-based compounds", *Applied Surface Science* **218**, 297-304 (2003).
- <sup>20</sup> J. H. Underwood, E. M. Gullikson, "High-resolution, high-flux, user friendly VLS beamline at the ALS for the 50-1300 eV energy region," *J. Electr. Spectr. Rel. Phenom.* **92**, 265-272 (1998).
- <sup>21</sup> E. M. Gullikson, S. Mrowka, B. B. Kaufmann, "Recent developments in EUV reflectometry at the Advanced Light Source," in *Emerging Lithographic Technologies.*, V. E. A. Dobisz ed., *Proc. SPIE* **4343**, 363-373 (2001).
- <sup>22</sup> B.L. Henke, E.M. Gullikson, and J.C. Davis. *X-ray interactions: photoabsorption, scattering, transmittance, and reflection at E=50-30000 eV, Z=1-92*, *Atomic Data and Nuclear Data Tables* **54** (2), 181-342 (1993); Database currently maintained by E. M. Gullikson, *X-Ray Interactions With Matter*, [http://henke.lbl.gov/optical\\_constants/](http://henke.lbl.gov/optical_constants/)

---

<sup>23</sup> J. Stöhr, *NEXAFS Spectroscopy* (Springer-Verlag, Berlin, 1992).

<sup>24</sup> M. Altarelli, D. L. Dexter, H. M. Nussenzveig and D. Y. Smith, “Superconvergence and Sum Rules for the Optical Constants”, *Phys. Rev. B* **6**(12) 4502-4509 (1972).